JPET Fast Forward. Published on January 25, 2005 as DOI: 10.1124/jpet.104.080457
JPET #80457

Mechanistic Pharmacokinetic and Pharmacodynamic Modeling of CHF3381, a Novel NMDA Antagonist and MAO-A Inhibitor in Healthy Subjects

Chantal Csajka, Bruno P. Imbimbo, Annalisa Piccinno, Philippe Dostert and Davide Verotta

Department of Biopharmaceutical Sciences, University of California, San Francisco, California (C.C., D.V.), Research & Development Department, Chiesi Farmaceutici, Parma, Italy, Biotrial (B.P.I., A.P.), Technopole Atalante Villejean, 7-9 rue Jean-Louis Bertrand, 35000 Rennes France (P.D.) and Department of Biostatistics, University of California, San Francisco, California (D.V.).

Running title: Mechanistic population PK-PD modeling of CHF3381

Corresponding Author:

Dr. Davide Verotta, PhD

Department of Biopharmaceutical Sciences and Biostatistics

University of California, Box 0446,

San Francisco, CA 94143

Tel: (415) 476 1556

Fax: (415) 476 1508

e-mail davide@ariel1.ucsf.edu

Number of page: 37

Number of tables: 3

Number of figures: 7

Number of references: 30

Number of words in the abstract: 204

Number of words in the Introduction: 358

Number of words in the Discussion: 1030

ABBREVIATIONS: MAO-A, monoamine oxidase-A; DHPG, 3,4-dihydroxyphenyl-glycol; NDMA receptors, N-methyl-D-aspartate receptors; CHF3381, 2-[(2,3-dihydro-1H-inden-2-yl) amino] acetamide monohydrochloride; CHF3567, N-(2,3-dihydro-1H-inden-2-yl)-glycine; 2-Aminoindane, 2,3-dihydro-1H-inden-2-amine.

JPET Fast Forward. Published on January 25, 2005 as DOI: 10.1124/jpet.104.080457
This article has not been copyedited and formatted. The final version may differ from this version.

Abstract

CHF3381 is a new N-methyl-D-aspartate (NMDA) antagonist and reversible monoamine oxidase-A (MAO-A) inhibitor in development for the treatment of neuropathic pain. This study developed a mechanistic model to describe the pharmacokinetics of CHF3381 and of its two metabolites, the relationship with MAO-A activity and heart rate. Doses of 100 mg, 200 mg and 400 mg twice daily for two weeks were administered orally to 36 subjects. MAO-A activity was estimated by measuring concentrations of 3,4-dihydroxy-phenylglycol (DHPG), a stable metabolite of norepinephrine. A multi-compartment model with time-dependent clearance was used to describe the kinetics of CHF3381 and metabolites concentrations. Estimated pharmacokinetic parameters were CL (43.0 L/h to 27.5 L/h over the study), V (133 L), Q (1.7 L/h), V_p (40 L) and ka (1.86 h^{-1}). The relationship between CHF3381 and DHPG or heart rate was described using an indirect or a direct linear model, respectively. The production rate of DHPG (k_{in}) was 2540 $ng \cdot h^{-1}$, reduced by 63 % at maximal CHF3381 concentrations. EC_{50} was 1,670 µg/L, not significantly different from the *in vitro* IC_{50}. The increase in heart rate due to CHF3381 was 0.0055 bpm/µg L^{-1}. CHF3381 produces a concentration-dependent decrease in DHPG plasma concentrations, whose magnitude increased after multiple twice-a-day regimens for 14 days.

Introduction

Neuropathic pain is defined as pain initiated or caused by a primary lesion or dysfunction in the nervous system (Merskey and Bogduk, 1994). The primary lesion or dysfunction can occur at any point along the sensory pathway: peripheral nerve, dorsal root ganglion or central nervous system. Anticonvulsants, tricyclic antidepressants and membrane stabilizers are widely used in neuropathic pain but the available evidence regarding their effectiveness is sparse (McCleane, 2003). It is believed that N-methyl-D-aspartate (NMDA) receptors are involved in the mechanism of pain hypersensitivity occurring in the neurons of dorsal horns of spinal cord ("central sensitization") that leads to chronic neuropathic pain (Woolf et al., 2004). Indeed, high affinity NMDA receptor antagonists like ketamine (Eide et al., 1995) or dextromethorphan (Carlsson et al., 2004) have been shown to reduce pain in patients with neuropathic pain but unfortunately their use was associated to unacceptable psychomimetic side effects. Development of drugs that block central sensitization without major adverse events is being actively pursued.

CHF3381 is a new low-affinity, uncompetitive NMDA antagonist and monoamine MAO-A (MAO-A) inhibitor under development for the treatment of neuropathic pain (Villetti et al., 2001; Zucchini et al. 2002). Pharmacological studies have shown that CHF3381 is active in a variety of rodent models of acute, inflammatory and neuropathic pain (Villetti et al. 2003). The NMDA antagonism of CHF3381 is believed to antagonize the central sensitization component of neuropathic pain while the MAO-A inhibition contributes to the antinociceptive activity (Gandolfi et al. 2001; Barbieri et al. 2003). The pharmacokinetics of CHF3381 in healthy volunteers has been described after single oral administration (Tarral et al. 2003). The aim of the present study is to define the

population pharmacokinetic-pharmacodynamic modeling of CHF3381 after multiple oral doses in healthy volunteers. The pharmacokinetics of CHF3381 and of its two major metabolites, CHF3567 and 2-aminoindane, were simultaneously modeled. MAO-A activity in plasma was estimated by measuring concentrations of 3,4-dihydroxy-phenyl-glycol (DHPG) and the concentration-effect relationship between CHF3381 and DHPG concentrations was characterized. In addition, an *in vitro/in vivo* correlation between CHF3381 concentrations an MAO-A inhibition was established using a Bayesian approach. Finally, a relationship between CHF3381 plasma concentrations and supine heart rate was described.

Material and Methods

Study Design

Data were derived from a double-blind, randomized, placebo-controlled, parallel group study of multiple oral doses of CHF3381 in young healthy male volunteers. Forty-eight healthy volunteers were enrolled in the study. Sixteen subjects were randomized in each of three dose panels to receive multiple oral dose of either CHF3381 (12 subjects) or placebo (4 subjects) administered in capsules. The dose regimens of CHF3381 were 100, 200 and 400 mg once-a-day at *Day 1*, 100, 200 and 400 mg twice-a-day (b.i.d) from *Day 2* to *Day 13* and 100, 200 and 400 mg once-a-day on *Day 14*. Subjects were asked to abstain from consuming alcoholic beverages from 48 hours before administration of study medication and throughout the 17-day inpatient stay. The study was carried out at Biotrial, Rennes (France) and the study protocol approved by the Rennes Institutional Review Board (Comité consultatif de protection des personnes dans la recherche

biomédicale de Rennes). Signed and dated written informed consent was obtained from all subjects.

Pharmacokinetic Assessments

Venous blood samples (7 mL) were collected immediately prior to the dose and 0.5, 1, 2, 3, 4, 6, 8, 10, 12, 16, and 24 hours on *Day 1*, just before the morning dose on *Day 3*, *Day 5*, *Day 8* and *Day 11* and pre-dose and 0.5, 1, 2, 3, 4, 6, 8, 10, 12, 16, 24, 36 and 48 hours on *Day 14*. Blood was collected into heparinized tubes and immediately centrifuged at 1500 × g for 20 min at 4°C. Plasma was separated and frozen at -20°C until assayed. Two urine aliquots (10 mL) were collected just before study drug administration. At Day 1, urine was collected over the 0-12 and 12-24 hour periods. At Day 14, urine was collected over the 0-12, 12-24, 24-48 and 48-72 hour intervals. The total amount of drug collected over each interval was used to determine renal clearances in the PK modeling. Plasma and urine concentrations of CHF3381 (2-[(2,3-dihydro-1H-inden-2-yl) amino] acetamide monohydrochloride) and of its two main metabolites, the acid derivative, CHF3567 (N-(2,3-dihydro-1H-inden-2-yl)-glycine) and 2-aminoindane (2,3-dihydro-1H-inden-2-amine) were determined at Chiesi Farmaceutici with a high performance liquid chromatography (HPLC) method with fluorescence detector (Tarral et al., 2003). Briefly, 1.0 mL of plasma or 0.1 mL of urine was added to the internal standard (N-[2-[(2,3-dihydro-1H-inden-2-yl)amino]ethyl]-acetamide, monohydrochloride) and 0.5 mL of 0.5 M phosphate buffer pH 11.7. The samples were extracted with 6 mL of a diethyl ether-butanol mixture (80:20) containing 0.3% tetra-n-octylammonium bromide. Then, 0.2 mL of 0.1 N HCl were added to the organic phase and 30 µL of the acidic phase were

injected into the HPLC system. Chromatographic separation was obtained using reversed phase HPLC, with retention times of 13.3 min for CHF 3381, 14.9 min for 2-aminoindane, 17.7 min for CHF 3567 and 18.5 min for the internal standard. The mobile phase contained 15 % methanol and 85 % 0.5 M phosphate buffer pH 2.7 and was pumped at a flow rate of 0.5 mL/min. The stationary phase was a C18 column (X-Terra MS, 150 x 4.6 mm, 3.5 µm, Waters, Milford, MA). Analytes were detected using a fluorescence HPLC detector (mod 474, Waters) set at 266 nm (excitation) and 286 nm (emission). The method was found to be linear in the 2-2,000 ng/mL plasma concentration range for CHF3381 and CHF3567 (20-20,000 ng/mL in urine), and in the 1-1,000 ng/mL range for 2-aminoindane (10-10,000 ng/mL in urine). The inter- and intra-day precisions were tested at 3 concentrations included in the concentration ranges. The precision and accuracy of the assay were measured at 3 concentrations included in the concentration ranges. Intra-day precision for the three compounds, expressed as coefficients of variation, ranged from 0.2 to 3.6 % in plasma and from 0.7 to 9.1 % in urine. Inter-day precision ranged from 3.1 to 7.6 % in plasma and from 2.3 to 6.3 % in urine. Intra-day accuracy, expressed as relative percent error, ranged from -3.5 to +5.9 % in plasma and from -8.9 to +3.0 % in urine. Inter-day accuracy ranged from –0.7 to 6.3 % in plasma and from –2.6 to 3.0 % in urine. Plasma and urine samples were suitably diluted with blank human matrix if the concentrations were greater than the highest standard sample of the corresponding calibration curves. The lower limit of quantitation in plasma was 2 µg/L for CHF3381 and CHF3567 and 1 µg/L for 2-aminoindane. The corresponding limits in urine were 20 µg/L and 10 µg/L, respectively.

Pharmacodynamic Assessments

MAO-A activity in plasma was estimated by measuring free plasma concentrations of 3,4-dihydroxyphenylglycol (DHPG), the deaminated metabolite of norepinephrine, which provide an indirect measure of the activity of the MAO-A enzyme. Venous blood samples (6.2 mL) for assay of DHPG concentrations were collected immediately prior to the dose and 1, 2, 3, 4, 6, 8, 12, 16, and 24 hours on *Day 1*, just before the morning dose on *Day 3*, *Day 5*, *Day 8* and *Day 11* and pre-dose and 1, 2, 3, 4, 6, 8, 12, 16, 24, 36 and 48 hours on *Day 14*. DHPG assays were performed at Cephac (Saint-Benoit, Cedex, France) a HPLC method with electrochemical detection (Patat et al., 1996). Briefly, the method used a fixation on alumina under basic conditions followed by washing with water and defixation under acid conditions. The extract was analyzed on a reversed phase column (Symmetry Shield ™, RP18, 100Å, 250 x 4,6mm, 5µ, Waters, Milford, Massachussets, USA). 3,4-dihydroxybenzylamine was used as internal standard. The method was linear in the 100 to 4,000 ng/L range. The limit of quantitation was 100 ng/L. Precision and accuracy were calculated at four concentrations (100, 250, 2000, 3500 ng/mL). The coefficient of variation of intra- and inter-day precision were lower than 9%. The relative percent error of intra- and inter-day accuracy was lower than ± 10%. Supine heart rate was measured 2 and 4 hours post-drug administration on *Day 1*, *Day 4*, *Day 10* and *Day 14* using Dynamap device (Pro-serie 100, GE Medical Information Technologies, Velizy, France).

JPET Fast Forward. Published on January 25, 2005 as DOI: 10.1124/jpet.104.080457
This article has not been copyedited and formatted. The final version may differ from this version.

Pharmacokinetics Modeling

CHF3381 pharmacokinetics were characterized using a eight-compartment model (see Figure 1). The model is described by the following differential equations which express the mass (amount) balance for each of the 8 compartments.

$$\begin{aligned}
&\frac{dA}{dt} = -ka\,A \\
&\frac{dC}{dt}V = ka\,A - (CL+Q)C + Q\,C_p \\
&\frac{dC_p}{dt}V_p = QC - Q\,C_p \\
&\frac{dM_1}{dt}V_{M_1} = f_{24}CL\,C - CL_{M_1}\,M_1 \\
&\frac{dM_2}{dt}V_{M_2} = f_{25}CL\,C - Vm\,M_2/(km+M_2) - CL_{R_{M_2}}M_2 \\
&\frac{dU}{dt} = CL_R\,C \\
&\frac{dU_1}{dt} = CL_{RM_1}\,M_1 \\
&\frac{dU_2}{dt} = CL_{R_{M_2}}\,M_2
\end{aligned} \qquad (1)$$

Where A, is the amount of CHF3381 in the absorption compartment, C, M_1 and M_2 are the measured concentrations of CHF3381, CHF3567 and 2-aminoindane, respectively, C_p is the (unmeasured) concentrations of CHF3381 in the peripheral compartment. U, U_1 and U_2 are the amounts of CHF3381, CHF3567 and 2-aminoindane in urine, respectively. ka is the first order absorption rate constant, CL clearance, Q inter-compartmental clearance, and V and V_p the volume of distribution for the central and peripheral compartment, respectively, CL_{M_1} is CHF3567 clearance, Vm is the maximal elimination rate for 2-aminoindane and km is the concentrations yielding 50% Vm, f_{xy} $(0 \le f_{xy} \le 1)$) is the fraction of the total mass that goes from compartment x to y, CL_R, $CL_{R_{M_1}}$ and

JPET Fast Forward. Published on January 25, 2005 as DOI: 10.1124/jpet.104.080457
This article has not been copyedited and formatted. The final version may differ from this version.

$CL_{R_{M_2}}$ are renal clearances for CHF3381, CHF3567 and 2-aminoindane, respectively. Initial conditions are $A(0) = dose\ F$, where F is bioavailability, and zero for the other compartments. Since F could not be identified in absence of intravenous drug administration, CL, and V are apparent values (e.g. $CL = CL^{true}/F$, where CL^{true} is the true clearance). Similarly the volume terms for M_1 and M_2 incorporate additional unknown fractions[1].

We used three different kinds of models to describe an observed change in clearance between the first and last dose administration. The first kind relates clearance to time elapsed from the first dose (Levy et al., 1976) as follows:

$$CL = CL_{ss} - (CL_{ss} - CL_B)e^{-k_{CL}t} \qquad (2)$$

The initial value of clearance (CL_B) reaches CL_{ss} exponentially, with rate constant k_{CL}. To test if drug exposure is affecting clearance we also allowed different CL_{ss} and k_{CL} depending on dose. The model was implemented using indicator variables:

$$CL_{ss} = CL_1 I_1(dose) + CL_2 I_2(dose) + CL_3 I_3(dose) \qquad (3)$$

$$k_{CL} = k_{CL1} I_1(dose) + k_{CL2} I_2(dose) + k_{CL3} I_3(dose) \qquad (4)$$

[1] It might be of interest to show the relationship between the estimated parameters and the unknown bioavailability and fractions of mass transfer between compartments. The relationships (which can be obtained by converting equation (1) into amounts) are as follows:

$$ka = ka^{true}$$
$$V = V^{true}/F$$
$$CL = CL^{true}/F$$
$$Q = Q^{true}/F$$
$$V_p = V_p{}^{true}/F$$
$$V_{M_1} = V_{M_1}{}^{true}/F/f_{24}$$
$$CL_{M_1} = CL_{M_1}{}^{true}/F/f_{24}$$
$$V_{M_2} = V_{M_2}{}^{true}/F/f_{25}$$
$$Vm = Vm^{true}/F/f_{25}$$
$$km = km^{true}/F/f_{25}$$
$$CL_R = CL_R{}^{true}/F/f_{26}$$
$$CL_{RM_1} = CL_{RM_1}{}^{true}/F/f_{24}/f_{47}$$
$$CL_{R_{M_2}} = CL_{R_{M_2}}{}^{true}/F/f_{25}/f_{58}$$

where F and the f_{xy}s are not identifiable.

JPET Fast Forward. Published on January 25, 2005 as DOI: 10.1124/jpet.104.080457
This article has not been copyedited and formatted. The final version may differ from this version.

where $I_1(dose)$, $I_2(dose)$, $I_3(dose)$ are 1 when dose is 100 mg, 200 mg and 400 mg, respectively, and zero otherwise.

The second class of models relates clearance to drug exposure as follows:

$$CL = CL_{ss} - (CL_{ss} - CL_B)\, f(A_T) \tag{5}$$

where $A_T(t) = \int_0^t A(t)\ dt$, represents the cumulative exposure (dose) of CHF3381 through the absorption compartment. We tested:

$$f(A_T) = 1 - \frac{A_T}{A_T + A_{T,50}} \tag{6}$$

$A_{T,50}$ is the exposure of CHF3388 that half the difference $CL_{ss} - CL_B$, and

$$f(A_T) = 1 - \frac{A_T^{\gamma}}{A_T^{\gamma} + A_{T,50}^{\gamma}} \tag{7}$$

where γ is a parameter determining the steepness of the curve.

(Additional models attempted to relate clearance to CHF3381 plasma concentration according to $CL = CL_B - (CL_B - CL_{ss})\frac{C}{C + EC_{50}}$, or, as suggested by a reviewer, $CL = CL_B + \frac{V_m}{C + Km}$. These clearance models did not achieve satisfactory results.) The inter-compartmental clearance (Q) was always adjusted to decrease by the same proportion of clearance. Derived pharmacokinetic parameters were initial half-life $\frac{\ln(2)}{\lambda_1}$ and terminal half-life $\frac{\ln(2)}{\lambda_2}$, where λ_1 and λ_2 are rate constants associated with the initial and the terminal phases, respectively, and absorption half-life as $\frac{\ln(2)}{ka}$.

Pharmacodynamic Modeling

Different kinds of models were tested to assess the effect on CHF3381 on the two pharmacodynamic variables: DHPG concentrations as a surrogate marker of MAO-A inhibition and heart rate. The simplest are linear models of the form:

$$E(t) = E_0(1+\alpha Z(t)) \qquad (8)$$

where E(t), with abuse of notation, indicates the effect at time t of CHF3381 on DHPG concentrations or on the increase in heart rate, E_0 is the baseline DHPG level or heart rate, α is the fractional change in E_0 due to Z(t), and $Z(t) = C(t)$, that is CHF3381 concentration, or $Z(t) = Ce(t)$ where *Ce(t)* is the concentrations of CHF3381 in an hypothetical effect compartment described by the following equation (Segre, 1968):

$$\frac{dCe(t)}{dt} = keo\left(C(t) - Ce(t)\right); \quad Ce(0) = 0 \qquad (9)$$

where *keo* is the first order rate constant from plasma to effect compartment. The assumption that baseline heart rate values remain constant without drug administration was based on the pharmacodynamic plot of heart rate vs. time after placebo administration (not shown) which did not show any major fluctuation in heart rate over the study period.

Second, we used a non-linear model of the form:

$$E(t) = E_0\ (1+\alpha \frac{Z(t)}{Z(t)+EC_{50}}) \qquad (10)$$

where EC_{50} is the concentration yielding half of the fractional maximal change in α.

For DHPG we also use an indirect model (Jusko and Ko, 1994) which describes the rate of change of effect as a function of Z(t):

JPET Fast Forward. Published on January 25, 2005 as DOI: 10.1124/jpet.104.080457
This article has not been copyedited and formatted. The final version may differ from this version.

$$\frac{dE}{dt} = k_{in}(1-\alpha\frac{Z(t)}{Z(t)+EC_{50}}) - k_{out}E \quad ; E(0) = \frac{k_{in}}{k_{out}} \tag{11}$$

where k_{in} is the zero order production rate of DHPG and k_{out} its elimination rate constant, α now symbolizes, with abuse of notation, the fractional decrease in k_{in}.

To account for the observed baseline reduction of DHPG concentrations at the end of day 14 of the study (100, 200 and 400 mg repeated doses induce a 5%, 8% and 15% baseline reduction, respectively), we introduce a time-varying baseline, $E_o(t)$, as follows:

$$E_o(t) = E_0\left[1-(1-\beta)\frac{A_T(t)}{A_T(t)+AC_{50}}\right] \tag{12}$$

where A_T is the solution to $\frac{dA_T}{dt} = kaA$ (i.e. the total absorbed dose), and β and AC_{50} are parameters characterizing the decrease in baseline due to total drug absorbed at any time. Equation 10 is now:

$$E(t) = E_0(t)\left[1-\alpha\frac{Z(t)}{Z(t)+EC_{50}}\right] \tag{13}$$

and similarly equation (11) becomes:

$$\frac{dE}{dt} = k_{in}E_0(t)\left[1-\alpha\frac{Z(t)}{Z(t)+EC_{50}}\right] - k_{out}E \;; E_t(0) = \frac{k_{in}}{k_{out}}. \tag{14}$$

Statistical Model

A hierarchical model was used to account for interindividual and intraindividual variability, as implemented in the NONMEM software (Boekmann et al., 1992). The individual pharmacokinetic and pharmacodynamic parameters θ_j were modeled assuming a log normal distribution and were of the general form:

$$\theta_j = \theta\ e^{\eta_j} \tag{15}$$

JPET Fast Forward. Published on January 25, 2005 as DOI: 10.1124/jpet.104.080457
This article has not been copyedited and formatted. The final version may differ from this version.

where θ is the population mean, and η_j are independent normally distributed effects with mean zero and variance Ω.

We used a proportional error model to describe intraindividual (residual) variability for CHF3381, CHF3567 and 2-aminoindane concentrations, their amounts in urine and the pharmacodynamic effects. For the generic response Y and the corresponding prediction $\hat{Y}$, the i^{th} measurement for the j^{th} individual takes the form:

$$Y_{ji} = \hat{Y}(1+\varepsilon_{ji}) \qquad (16)$$

where ε_{ij} is independent normally distributed with mean zero and a variance σ^2.

Parameter Estimation and Model Selection

We used NONMEM VI with FOCE INTERACTION and 3 significant digits to fit the models described above to the data. The compiler is the SunPro FORTRAN 77 running on a Sun Workstation Ultra-5. We used a sequential PK/PD analysis: first the pharmacokinetic model for CHF3381, CHF3567 and 2-aminoindane was established fitting simultaneously all the plasma concentration and urine data. Second, conditional on the individuals empirical Bayes estimates corresponding to the final model (obtained using the NONMEM option POSTHOC), the pharmacodynamic data were fitted. (In general we prefer a sequential analysis for PD data to protect against model misspecification. Simulations studies (Zhang et al., 2003) have shown that sequential and simultaneous analyses perform similarly.

To determine the statistical significance between two models, one can use different statistical selection criteria (Akaike, 1974; Hannan, 1987; Schwartz, 1978) which require a minimal decrease of 2 to 10 points in the objective function (minus twice the logarithm of the linearized maximum likelihood of the model) to accept a model with one additional

parameter. The minimum drop in the objective function observed in our model selection process was 30 points (see Results). Representative individuals corresponding to the 5^{th} ("best" fit) and 95^{th} ("worst" fit) percentile of the distribution of the sum of the squared individual weighted residual were plotted, together with other diagnostic plots (predictions vs. time).

For the pharmacodynamic responses in addition to the maximum-likelihood estimates we also obtained Bayesian estimates for model parameters (Gelman et al. 1995) using NONMEM VI (see Gisleskog et al., 2002). To do so we used the *in vitro* affinity of CHF3381 for the human MAO-A enzymes, and its SE, to define a prior normal distribution for EC_{50}. This is a statistically sound method to establish *in-vitro/in-vivo* correlation and we performed this additional analysis to show an example of such an application.

The final PK/PD population model was used to simulate desired statistics by sampling from the estimated distribution of the PK and PD parameters. In general, we generated N subjects and increased N until the statistic of interest (averaged over the N subjects) showed convergence. We used N=3000 for the minimum and maximum percent of inhibition, expressed as (baseline-DHPG level)/baseline of DHPG, in respect to each individual baseline reported in the results section below. The desired DHPG levels were obtained as follows: after a steady-state dose, for each simulated individual, the maximum degree of inhibition is determined by a grid search with resolution of 0.5 hours over the inter-dose interval, the minimum degree of inhibition is observed immediately after the dose.

Variances and standard errors (SE) of the estimates are expressed as coefficients of variation (CV %). The figures were generated with S-PLUS (Statistical Sciences, Version 4.0 Release 2 1997).

Results

Forty-eight male subjects were enrolled in the study. All subjects completed the study: 12 received placebo, 12 received 100 mg twice a day, 12 received 200 mg twice a day and 12 received 400 mg twice a day. Their median age was 26 years (range 20-36), their mean weight was 71.8 kg (range 59-86) and their mean body max index was 22.6 kg/m² (range 18.7- 27.4 kg/m²).

Pharmacokinetics

Plasma CHF3381, CHF3567 and 2-aminoindane concentrations ranged from 2.3 to 3893.1 μg/L, from 2.1 to 3381.4 μg/L, and from 0.8 to 438.4 μg/L, respectively. Urine CHF3381, CHF3567 and 2-aminoindane amounts ranged from 21–46338 μg, 146-259878 μg and 84-25658 μg, respectively.

A two-compartment model with first-order absorption described the data better than a one-compartment model, the decrease in the objective function (ΔOBJ) being -74. Introduction of a lag-time improved significantly the fits (ΔOBJ = -101). A fit of Day 1 and Day 14 data separately revealed a difference in clearance of 23% , while the volume of distribution, the absorption rate constant and the lag time remained constant. The model including a time-variant clearance (equations 2) resulted in a significant improvement of the fits (ΔOBJ = -416). The clearance was reduced from 43.0 L/h to 27.5

L/h (36 % inhibition) with rate constant k_{CL} of 0.14 h^{-1}. The two models with exposure-dependant clearance (equations 5, 6, 7) improved the fits significantly (ΔOBJ = -317, -328, respectively) but less than equation 2. The value of $A_{T,50}$ was estimated to be 100 μg by model (6) and 250 μg by model (7). The models using equations (3) and (4) revealed very similar values of k_{CL1}, k_{CL2}, and k_{CL3} (0.130, 0.133, and 0.125 h^{-1}) and CL_1, CL_2, and CL_3 (23.6, 24.1 and 23.2) which correspond to the dosage regimens of 100 mg, 200 mg and 400 mg, respectively, this indicating no dose dependency in clearance reduction. The model estimates 4.1 %, of dose excreted in urine. The final parameters estimates for CHF3381 are presented in table I.

A one compartment model with linear elimination adequately fit CHF3567 (M_1) data. Similarly, a one compartment model was used to fit 2-aminoindane (M_2) data. Owing to an observed accumulation of drug at the 400 mg dose, we introduced a non-linear (Michaelis-Menten) elimination for that metabolite, which improved significantly the fit (ΔOBJ = -134) compared to the linear model. The final parameters estimates for M_1 and M_2 are also presented in table I. Figures 2, 3 and 4 depict the observed plasma concentrations (open circles) the population predictions (solid line) and the predictions at steady-state levels (dashed line) over the whole study period for CHF3381, CHF3567 and 2-aminoindane after administration of 100 mg (upper panel), 200mg (middle panel) and 400mg (lower panel), respectively. Plasma concentrations (open circles) and the population predictions (solid line) of representative individuals at the 5^{th} and 95^{th} percentile of the sum of the individual weighted residual at the 200 mg dose level of CHF3381 are presented in figure 5.

Pharmacodynamics

DHPG plasma concentrations and heart rate values measured after administration of placebo did not show any regular fluctuation in this study (confirming the lack of significant diurnal variations in DHPG plasma concentrations reported in (Dennis et al., 1986; Patat et al., 1996))

The relationship between CHF3381 and the reduction of DHPG concentrations was first described by a simple linear model (see equation 8). The slope and the intercept of the linear regression were -0.28 and 872 ng/L, respectively. The addition of an effect compartment to account for a delay between the concentrations and the effects did not improve the fit of the data. The concentration-effect relationship appeared to be slightly non-linear at the highest concentrations and the use of an E_{max} model (equation 10) improved significantly the fits (ΔOBJ = -30). The estimated value of the maximal fractional decrease α (0.99) as a function of CHF3381 concentrations was not statistically different from one and was thus fixed to this value. The indirect model (equation 11) showed a marked improvement of the fits (ΔOBJ = -101). To account for the observed residual inhibition of the MAO-A activity observed at time 36 to 48 hours after drug intake on *Day 14* (approximately 5 %, 8 % and 15% for dose 100, 200 and 400 mg respectively), we modeled the baseline DHPG concentration as a function of the drug exposure using models (13) or (14). Both models successfully described the data and significantly improved the fits (ΔOBJ = -130 and -184, respectively). For both models, a 15 % reduction in the baseline DHPG concentration (E_0) was observed.

The in vitro CHF3381 IC_{50} for MAO-A enzyme affinity is 7.8 mM (SE = 1mM), corresponding to IC50 = 1768 (SE = 227) mg/L [Gandolfi et al., 2001]. IC50 and it standard error were used to define a prior normal distribution for *in-vivo* EC_{50} obtaining the corresponding (Bayesian) estimates for the pharmacodynamic model: k_{in} = 2560 ng/Lh^{-1}, k_{out} = 2.6 h^{-1}, EC_{50} = 1680 μg/L, AC_{50} = 238 mg, α = 1 and β = 0.85. Comparing IC_{50} and EC_{50} shows a high degree of *in-vitro/in-vivo* correlation. Since Bayesian estimation might not be familiar to many readers, for comparison we also report the standard maximum likelihood estimates which are very similar: k_{in} = 2540 ng/Lh^{-1}, k_{out} = 2.53 h^{-1}, EC_{50} = 1670 μg/L, AC_{50} = 241 mg, α = 1 and β = 0.85 (see also table III).

The final PK/PD population model was used to simulate the population distribution of DHPG concentrations. For the drug regimens of 100, 200, 400 and 800 mg dose twice daily, significant quantiles of the minimum and maximum percent of inhibition of DHPG in respect to each individual baseline were computed and are presented in table II. These results confirm the high degree of inhibition of DHPG levels at all doses, the extrapolation to the 800 mg dose regimen suggests that higher degrees of inhibition can be achieved by increasing the dose.

The relationship between CHF3381 concentrations and heart rate was successfully described using a linear model. No other pharmacodynamic model obtained a better fit to the data. We estimated an increase in heart rate of 0.0055 bpm/μg/L due to CHF3381. The population estimates and variances of the final pharmacodynamic parameters are presented in table III. Figures 6 depicts the observed plasma concentrations (open circles), with the population predictions (solid line) over the whole study period for the effect of

CHF3381 on DHPG concentrations after administration of 200mg CHF3381 and figure 7 represents the concentration-effect relationship of CHF3381 on heart rate.

Discussion

CHF3381 pharmacokinetics was characterized by the inhibition of clearance over time. This effect could not be modeled using either dose-dependent or exposure-dependent elimination. Whether this characteristic is related to auto-inhibition or to interference of metabolites or other substances in the elimination pathway of CHF3381 need to be further addressed. The initial and terminal half-lives of CHF3381 after multiple dose administration were 3.2 h and 18 h respectively, and the absorption half-life was 23 minutes with a lag time of 11 minutes. A large inter-subject variability in the absorption profile of CHF3381 was observed and might be related to some food interaction, known to influence the rate of absorption of CHF3381 (Tarral et al., 2003). A rather high residual intra-subject variability in CHF3381 plasma and urine data was estimated by NONMEM.

CHF3381 was linearly metabolized into its two major metabolites CHF3567 and 2-aminoindane. We observed a rapid onset of inhibition of its total clearance (the half-life for the decrease of clearance to its steady-state value ($0.693/ k_{CL}$) is about 5 hours according to our final model). 2-aminoindane showed a dose-dependant accumulation over time which suggested saturable elimination. Although the introduction of a saturable elimination clearly improved the fits, a slight misfit in the population predicted concentrations of 2-aminoindane at day 14 of the study at the highest concentrations for the lower doses remained visible (see figure 4). The individual fits were however satisfactory (data not shown), suggesting a small unexplained bias in the population

estimates. The accumulation of 2-aminoindane may explain the previously reported minor sympathicomimetic effects of this drug (Mrongovius et al., 1978). Renal clearance accounts for only a small part of CHF3381 elimination, the fraction of the dose recovered in urine being 4%. This result is in good agreement with our previously published value of 2% to 6% of the administered dose excreted in the urine (Tarral et al., 2003). In this study, MAO-A activity was estimated by measuring DHPG concentrations in plasma, a stable metabolite of norepinephrine. This approach assumes that DHPG clearance is constant and that the input of norepinephrine is constant. Several studies have shown that plasma DHPG concentrations are a good marker of the magnitude and duration of MAO-A inhibition in humans (Patat et al., 1996; Dingemanse et al., 1996; Bitsios et al., 1998; Scheinin et al., 1998). The inhibitory effect of CHF3381 on DHPG plasma concentrations was successfully described using an indirect action model, with CHF3381 acting on the formation rate of DHPG. A direct action model using an effect site compartment did not fit the data as well. Similarly to other reversible and selective MAO-A inhibitors (Bieck et al., 1993) like moclobemide (Holford NH et al., 1994), befloxatone (Patat et al., 1996), brofaromine (Gleiter et al., 1994) and toloxatone (Berlin et al., 1990), CHF3381 produces a dose-dependent inhibition of DHPG concentrations in plasma. The magnitude and the duration of the decrease in DHPG plasma concentrations were increased at steady state after multiple twice-a-day regimens for 14 days. Pre-dose trough inhibitions were observed both after the 200 mg (16 ± 4%) and the 400 mg (39 ± 6%) twice-a-day regimen indicating that twice-a-day administration well covers the 24-hour period. Observed drug effect was non-linearly related to CHF3381 dose and plasma concentrations, approaching a maximum at the highest concentrations. The asymptotic

100% reduction predicted by the model should be considered a, probably unreliable, extrapolation since observed and predicted CHF3381 concentrations were not far from the estimated value of EC_{50}, which fells into the concentration range of the 200 and 400 mg doses. Using the predicted maximal CHF3381 concentrations following the 100 mg, 200 mg and 400 mg dose, we estimate a 29 %, 50 % and 63 % reduction of the production rate of DHPG, respectively. Our modeling also indicated that the small fractional decrease in the baseline level of DHPG concentrations observed at the end of the two weeks long experiment can be related to a reduction in k_{in} associated to total amount of drug absorbed. We estimated a maximal 15% reduction (corresponding to the estimated parameter $\beta = 0.85$), but obtain an estimate for AC_{50} that is small compared to the total amount of drug administered after any of the three dose regimen. This implies that the maximal decrease in baseline after the 100 and 200 mg dose was slightly over predicted by our modeling (observed decrease in baseline for these two doses is below 10%). The mechanism for this small residual decrease in baseline DHPG plasma concentrations is unclear. In vitro, there are no indications for adduct or product formation after incubation of CHF3381 with MAO-A (Gandolfi et al., 2001). Even though, CHF3381 could have the characteristics of a slow-binding inhibitor, similarly to what described for moclobemide (Cesura et al., 1992), thus explaining the longer pharmacological activity compared to than what expected from its plasma half-life.

There is a good agreement between the inhibitory potency of CHF3381 on MAO-A estimated *in vivo* through DHPG inhibition and that determined *in vitro* using the purified human liver enzyme. *In vitro*, CHF3381 shows an IC_{50} of 7.8 (1.0) μM (1,768 (227) μg/L) (Gandolfi et al., 2001), a value very close to the EC_{50} for DHPG concentrations we

found in this study (1,670 (130) μg/L). CHF3381 interacts with the MAO-A enzyme and the NMDA ion channels with similar affinity (IC_{50}s of 7.8 μM and 8.1 μM, respectively) (Gandolfi et al., 2001) and thus plasma concentrations around 1,800 μg/L should produce significant NMDA occupancy. These plasma concentrations were exceeded in this study with the 400 mg twice-a-day dose regimen, suggesting that this dose regimen should produce a pharmacological effect.

A small linear effect between CHF3381 and heart rate was observed, indicating an increase of 5.5 bpm with each 100 μg/L of CHF3381.

In conclusion, we described the population pharmacokinetic-pharmacodynamic relationship of CHF3381 after repeated drug administration in healthy volunteers. CHF3381 produced a dose-dependent inhibition of MAO-A activity, as estimated through inhibition of DHPG plasma levels. There was an excellent agreement between the *in vitro* affinity of CHF3381 for the MAO-A enzyme and EC_{50} we found in this study on DHPG plasma levels, suggesting that DHPG is a good marker for estimating MAO-A inhibitory activity of CHF3381 *in vivo*.

References

Akaike A (1974) A new look at the statistical model identification problem. *IEEE Trans Autom Contr* 19:716-723.

Barbieri M, Bregola G, Buzzi A, Marino S, Zucchini S, Stables JP, Bergamaschi M, Pietra C, Villetti G, Simonato M (2003) Mechanisms of action of CHF3381 in the forebrain. *Br J Pharmacol* 139: 1333-1341.

Berlin I, Zimmer R, Thiede HM, Payan C, Hergueta T, Robin L, Puech AJ (1990) Comparison of the monoamine oxidase inhibiting properties of two reversible and selective monoamine oxidase-A inhibitors moclobemide and toloxatone, and assessment of their effect on psychometric performance in healthy subjects. *Br J Clin Pharmacol* 30: 805-816.

Bieck PR, Antonin KH, Schmidt E (1993) Clinical pharmacology of reversible monoamine oxidase-A inhibitors. *Clin Neuropharmacol* 16 (Suppl 2): S34-41.

Bitsios P, Langley RW, Tavernor S, Pyykko K, Scheinin M, Szabadi E, Bradshaw CM (1998) Comparison of the effects of moclobemide and selegiline on tyramine-evoked mydriasis in man. *Br J Clin Pharmacol* 45: 551-558.

Boekmann SL, Beal SL, Sheiner LB, editors (1992) NONMEM users' guides. San Francisco: NONMEM Project Group, University of California at San Francisco.

Carlsson KC, Hoem NO, Moberg ER, Mathisen LC (2004) Analgesic effect of dextromethorphan in neuropathic pain. *Acta Anaesthesiol Scand* 48: 328-336.

Cesura AM, Kettler R, Imhof R, Da Prada M (1992) Mode of action and characteristics of monoamine oxidase-A inhibition by moclobemide. *Psychopharmacology* 106: S15-S16.

Dennis T, Benkelfat C, Touitou Y, Auzeby A, Poirier MF, Scatton B, Loo H (1986) Lack of circadian rhythm in plasma levels of 3,4-dihydroxyphenylethyleneglycol in healthy human subjects. *Psychopharmacology* 90: 471-474.

Dingemanse J, Kneer J, Wallnofer A, Kettler R, Zurcher G, Koulu M, Korn A (1996) Pharmacokinetic-pharmacodynamic interactions between two selective monoamine oxidase inhibitors: moclobemide and selegiline. *Clin Neuropharmacol* 19: 399-414.

Eide K, Stubhaug A, Oye I, Breivik H (1995) Continuous subcutaneous administration of the N-methyl-D-aspartic acid (NMDA) receptor antagonist ketamine in the treatment of post-herpetic neuralgia. *Pain* 61: 221-228.

Gandolfi O, Bonfante V, Voltattorni M, Dall'Olio R, Poli A, Pietra C, Villetti G (2001) Anticonvulsant preclinical profile of CHF 3381: dopaminergic and glutamatergic mechanisms. *Pharmacol Biochem Behav* 70: 157-166.

Gelman A, Carlin JB, Stern H, Rubin DB (1995) in *Bayesian Data Analysis*, London: Chapman and Hall.

Gisleskog PO, Karlsson MO, Beal SL (2002) Use of prior information to stabilize a population data analysis. *J Pharamcokin Pharmacodyn* 29(5):473-504.

Gleiter CH, Muhlbauer B, Schulz RM, Nilsson E, Antonin KH, Bieck PR (1994) Monoamine oxidase inhibition by the MAO-A inhibitors brofaromine and clorgyline in healthy volunteers. *J Neural Transm Gen Sect* 95: 241-245.

Holford NH, Guentert TW, Dingemanse J, Banken L (1994) Monoamine oxidase-A: pharmacodynamics in humans of moclobemide, a reversible and selective inhibitor. *Br J Clin Pharmacol* 37: 433-439.

Jusko WJ, Ko HC (1994) Physiologic indirect response models characterize diverse types of pharmacodynamic effects. *Clin Pharmacol Ther* 56(4):406-409.

Levy RH, Pitlick WH, Troupin AS, Green JR (1976) Pharmacokinetic interactions of chronic drug treatment in epilepsy: carbamazepine, in *The effects of Disease State on Drug Pharmacokinetics* (Ed. Benet L), Washington DC: Academy of Pharmaceutical Sciences pp 87-95.

McCleane G (2003). Pharmacological management of neuropathic pain. *CNS Drugs* 17: 1031-1043.

Merskey H, Bogduk N (1994) Classification of Chronic Pain, in *IASP Taskforce on Taxonomy,* 2nd Edition, IASP Press, Seattle pp 209-214.

Mrongovius RI, Bolt AG, Hellyer RO (1978) Comparison of the anorectic and motor activity effects of some aminoindanes, 2-aminotetralin and amphetamine in the rat. *Clin Exp Pharmacol Physiol* 5: 635-640.

Patat A, le Coz F, Dubruc C, Gandon JM, Durrieu G, Cimarosti I, Jezequel S, Curet O, Zieleniuk I, Allain H, Rosenzweig P (1996) Pharmacodynamics and pharmacokinetics of two dose regimens of befloxatone, a new reversible and selective monoamine oxidase inhibitor, at steady state in healthy volunteers. *J Clin Pharmacol* 36: 216-229.

Scheinin M, Illi A, Koulu M, Ojala-Karlsson P (1998) Norepinephrine metabolites in plasma as indicators of pharmacological inhibition of monoamine oxidase and catechol O-methyltransferase. *Adv Pharmacol* 42: 367-370.

Segre G. Kinetics of interaction between drugs and biological systems (1968) *Il Farmaco Ed Sci* 23: 907-918.

Tarral A, Dostert P, Guillevic Y, Fabbri L, Rondelli I, Mariotti F, Imbimbo BP (2003) Safety, pharmacokinetics and pharmacodynamics of CHF3381, a novel NMDA antagonist, after single oral doses in healthy subjects. *J Clin Pharmacol* 43: 901-911.

Villetti G, Bregola G, Bassani F, Bergamaschi M, Rondelli I, Pietra C, Simonato M (2001) Preclinical evaluation of CHF3381 as a novel antiepileptic agent. *Neuropharmacology* 40: 866-878.

Villetti G, Bergamaschi M, Bassani F, Bolzoni PT, Maiorino M, Pietra C, Rondelli I, Chamiot-Clerc P, Simonato M, Barbieri M (2003) Antinociceptive activity of the N-methyl-D-aspartate receptor antagonist N-(2-Indanyl)-glycinamide hydrochloride (CHF3381) in experimental models of inflammatory and neuropathic pain. *J Pharmacol Exp Ther* 306(2): 804-814.

Woolf CJ, American College of Physicians, American Physiological Society (2004) Pain: moving from symptom control toward mechanism-specific pharmacologic management. *Ann Intern Med* 140: 441-451.

Zhang L, Beal SL, Sheiner LB (2003) Simultaneous vs. sequential analysis for population PK/PD data I: best-case performance. *J Pharmacokin Pharmacodyn* 30(6):387-404.

Zucchini S, Buzzi A, Bergamaschi M, Pietra C, Villetti G, Simonato M (2002) Neuroprotective activity of CHF3381, a putative N-methyl-D-aspartate antagonist. *Neuroreport* 13: 2071-2074.

Footnotes

This study was sponsored by Chiesi Farmaceutici, Parma, Italy. This work was partly supported by the NIH grant A150587. Dr. C. Csajka was partly supported by a grant from the Swiss National Science Foundation.

Correspondence and Address for Reprints

Dr. Davide Verotta, PhD

Department of Biopharmaceutical Sciences and Biostatistics

University of California, Box 0446,

San Francisco, CA 94143

Tel: (415) 476 1556

Fax: (415) 476 1508

e-mail davide@ariel1.ucsf.edu

Legends for figures

Figure 1. Schematic representation of the pharmacokinetic compartmental model for CHF3381, CHF3567 and 2-aminoindane. A: absorption site CHF3381 amount; C: plasma CHF3381; C_p: peripheral CHF3381; M_1: plasma CHF3567; $M_{2:}$ plasma 2-aminoindane; $U_:$ urine CHF3381; U_1 urine CHF3567; U_2 urine 2-aminoindane. ka first order absorption rate constant, CL total clearance, Q inter-compartmental clearance, and V and V_p volume of distribution for the central and peripheral compartment, respectively, CL_{M1} CHF3567 clearance, Vm maximal elimination rate for 2-aminoindane, km concentrations yielding 50% Vm, f_{xy} $(0 \leq f_{xy} \leq 1)$) the fraction of the total mass that goes from compartment x to y, where zero indicates the outside of the model, CL_R, $CL_{R_{M_1}}$ and $CL_{R_{M_2}}$ are renal clearances for CHF3381, CHF3567 and 2-aminoindane, respectively. See also text.

Figure 2. Plasma concentrations (open circles) population prediction (solid line) and predictions at steady-state levels (dashed lines) for CHF3381 over the 14 days study period after administration of the 100 mg (upper panel) the 200 mg (middle panel) and the 400 mg dose regimens (lower panel).

Figure 3. Plasma concentrations (open circles), population prediction (solid line) and predictions at steady-state levels (dashed lines) for CHF3567 after administration of 100 mg (upper panel), 200 mg (middle panel) and 400 mg CHF3381 (lower panel).

Figure 4. Plasma concentrations (open circles), population prediction (solid line) and predictions at steady-state levels (dashed lines) for 2-aminoindane after administration of 100 mg (upper panel), 200 mg (middle panel) and 400 mg CHF3381 (lower panel).

Figure 5. Representative individuals at the 5^{th} (left panels) and 95^{th} (right panels) percentile of the weighted residual (WRES) distribution after 200 mg CHF3381.

Figure 6. Plasma concentrations of DHPG (open circles) and population predictions (solid lines) after administration of 200 mg CHF3381. The different prediction lines are the consequence of different individual pharmacokinetics.

Figure 7. Concentration-effect relationship of the measured CHF3381 levels *vs.* heart rate (open circles) and the population prediction (solid line).

JPET Fast Forward. Published on January 25, 2005 as DOI: 10.1124/jpet.104.080457
This article has not been copyedited and formatted. The final version may differ from this version.

Table I. Population estimates of the pharmacokinetic parameters of CHF3381, CHF3567 and 2-aminoindane.

Parameter	***Population Mean***		***Inter-subject Variability*** [a]	
	Estimate	*CV*[b]	*Estimate*	*CV*[c]
CHF3381				
CL_B (L/h)	43.0	9 %	9 %[g]	61 %
CL_{ss} (L/h)	27.5	9 %	9 %[g]	61 %
k_{CL} (h^{-1})	0.14	33 %		
ka (h^{-1})	1.86	33 %	165 %	67 %
Lag time (h)	0.2	12 %		
Q (L/h)	1.7	12 %		
V (L)	133	4 %	12 %	64 %
V_p (L)	40	6 %		
CL_R (% of CL)	4.1	9 %		
σ (CV%)[e]	46 %	5 %		
σ (CV%)[f]	67 %	8 %		
CHF3567				
CL_{M_1} (L/h)	3.4	3 %	16 %[g]	57 %
V_{M_1} (L)	76.7	5 %	16 %	79 %

JPET Fast Forward. Published on January 25, 2005 as DOI: 10.1124/jpet.104.080457
This article has not been copyedited and formatted. The final version may differ from this version.

$CL_{R_{M_1}}$ (L/h)	0.15	4 %	16 %[g]	57 %
σ (CV%)[e]	26 %	7 %		
σ (CV%)[f]	31 %	27 %		
2-aminoindane				
Vm (μg/h)	63.9	7 %	16 %[g]	50 %
km (μg/L)	256	9 %		
V_{M_2} (L)	3,410	3 %	11 %	64 %
$CL_{R_{M_2}}$ (L/h)	0.02	4 %	16 %[g]	50 %
σ (CV%)[e]	27 %	8 %		
σ (CV%)[f]	38 %	21 %		

CL_B, baseline clearance; CL_{ss}, clearance at steady-state; k_{CL}, rate constant for the decrease of clearance from clearance baseline to clearance at steady-state; ka, absorption rate constant, Q, inter-compartmental clearance, V, V_p, apparent volumes of distribution in the central and the peripheral compartment for CHF3381; V_{M_1}, V_{M_2}, apparent volume of distribution of M_1 and M_2, CL_{M_1}, clearance of M_1; Vm, maximal rate of elimination of M_2; km, concentration yielding 50 % of m_5; CL_R renal clearance for CHF3381, expressed as percent of total clearance (which changes over time, see text), $CL_{R_{M_1}}$, $CL_{R_{M_2}}$, renal clearance for CHF3567 and 2-aminoindane, respectively.

[a] Estimates of variability expressed as approximate coefficient of variation (CV%, $\sqrt{\Omega} \cdot 100$)

[b] Standard error of the estimates (SE), defined as $SE/estimate$, expressed as a percentage.

[c] Standard error of the coefficient of variation, taken as $\sqrt{SE_{estimate} / estimate}$, expressed a percentage.

[d] expressed as % of total clearance (at any time).

[e] Residual intra-subject variability of the plasma concentrations, expressed as coefficient of variation (CV%).

[f] Residual intra-subject variability of the urine amounts, expressed as coefficient of variation (CV%).

[g] The same random effect is associated with CL_B and CL_{ss}, CL_{M_1} and $CL_{R_{M_1}}$, Vm and $CL_{R_{M_2}}$, respectively.

JPET Fast Forward. Published on January 25, 2005 as DOI: 10.1124/jpet.104.080457
This article has not been copyedited and formatted. The final version may differ from this version.

Table II: Distribution of minimum and maximum percent of inhibition of baseline DHPG after steady-state administration of 100, 200, 400 and 800 mg twice daily of CHF3381 in simulated individuals.

Dose Regimen	100		200		400		800	
	min[a]	max[b]	min[a]	max[b]	min[a]	max[b]	min[a]	max[b]
Percentile								
5	23	37	29.9	49.8	40.6	64.1	54.5	76.9
25	18.4	35.9	21.9	48.5	28.1	62.7	37.9	75.7
50 (median)	17.4	34.6	19.9	46.8	24.6	61	32.6	74.4
75	16.8	31.3	18.8	42.5	22.7	56.6	29.4	70.8
95	16.2	26.6	17.8	35.6	20.8	48.3	26.1	63

The values corresponding to the percentiles listed in the first column are obtained simulating N=3000 subjects using the final population PK/PD model (see text).

[a] 100 (baseline minus concentration at time zero after dose)/baseline

[b] 100 (baseline minus minimum concentration during the inter-dose interval)/baseline.

The table entries should be read as we demonstrate for the first entry: 5% of the population receiving the 100 mg dose regimen has a minimum percent inhibition of 23% or higher.

JPET Fast Forward. Published on January 25, 2005 as DOI: 10.1124/jpet.104.080457
This article has not been copyedited and formatted. The final version may differ from this version.

Table III. Population estimates of the pharmacodynamic parameters of CHF3381.

Parameter	*Population Mean*		*Inter-subject Variability* [b]	
	Estimate	*SE*[c]	*Estimate*	*SE*[d]
DHPG conc. [a]				
k_{in} (ng h^{-1})	2540	19 %	20 %	76 %
k_{out} (h^{-1})	2.53	17 %	18 %	79 %
EC_{50} (μg/L)	1670	8 %	-	-
α [e]	1	-		
AC_{50} (mg)	241	38 %	109 %	81 %
β	0.85	4 %		
σ (CV %)[f]	14 %	13 %		
HR				
α/E_0 (bpm/μg L^{-1})	0.0055	18 %	66 %	70 %
E_0 (bpm)	59.9	2 %	8 %	45 %
σ (CV %)[f]	8 %	12 %		

k_{in}, zero order production rate of DHPG; k_{out}, elimination rate of DHPG; α, fractional decrease in k_{in}; EC_{50}, concentrations of CHF3381 at half of α; β, fractional decrease in baseline due to amount of CHF3381 absorbed, and AC_{50} total amount at half of β (see text).

[a] DHPG plasma concentrations were used as a marker of MAO-A enzyme activity.

[b] Estimates of variability expressed as approximate coefficient of variation (CV%, $\sqrt{\Omega} \cdot 100$)

[c] Standard error of the estimates, defined as $SE_{estimate}/estimate$, expressed as a percentage.

[d] Standard error of the coefficient of variation, taken as $\sqrt{SE_{estimate}/estimate)}$, expressed a percentage.

[e] fixed

[f] Residual intra-subject variability of the dynamic measure, expressed as coefficient of variation (CV %).

JPET Fast Forward. Published on January 25, 2005 as DOI: 10.1124/jpet.104.080457
This article has not been copyedited and formatted. The final version may differ from this version.

Figure 1

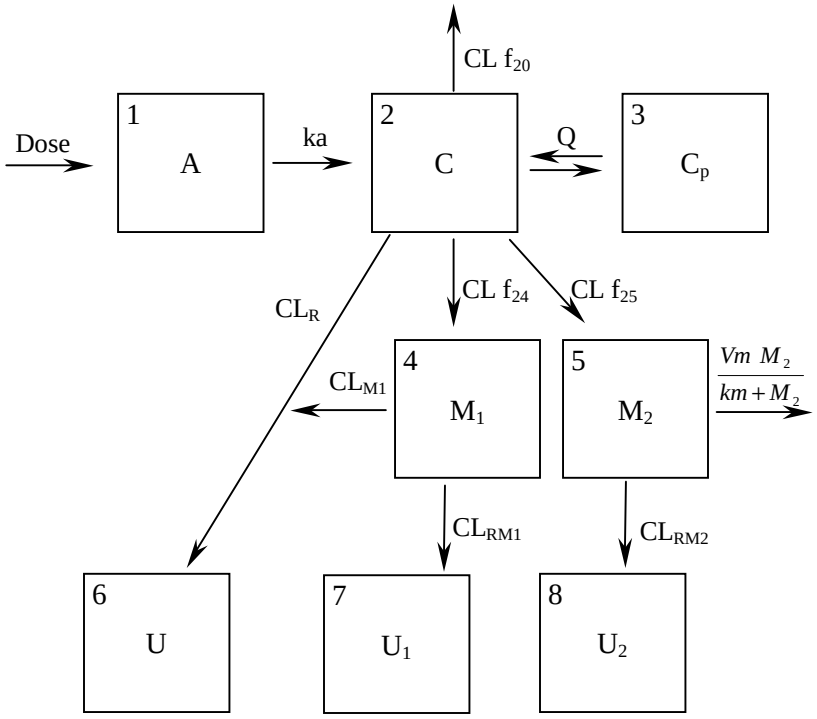

Figure 2

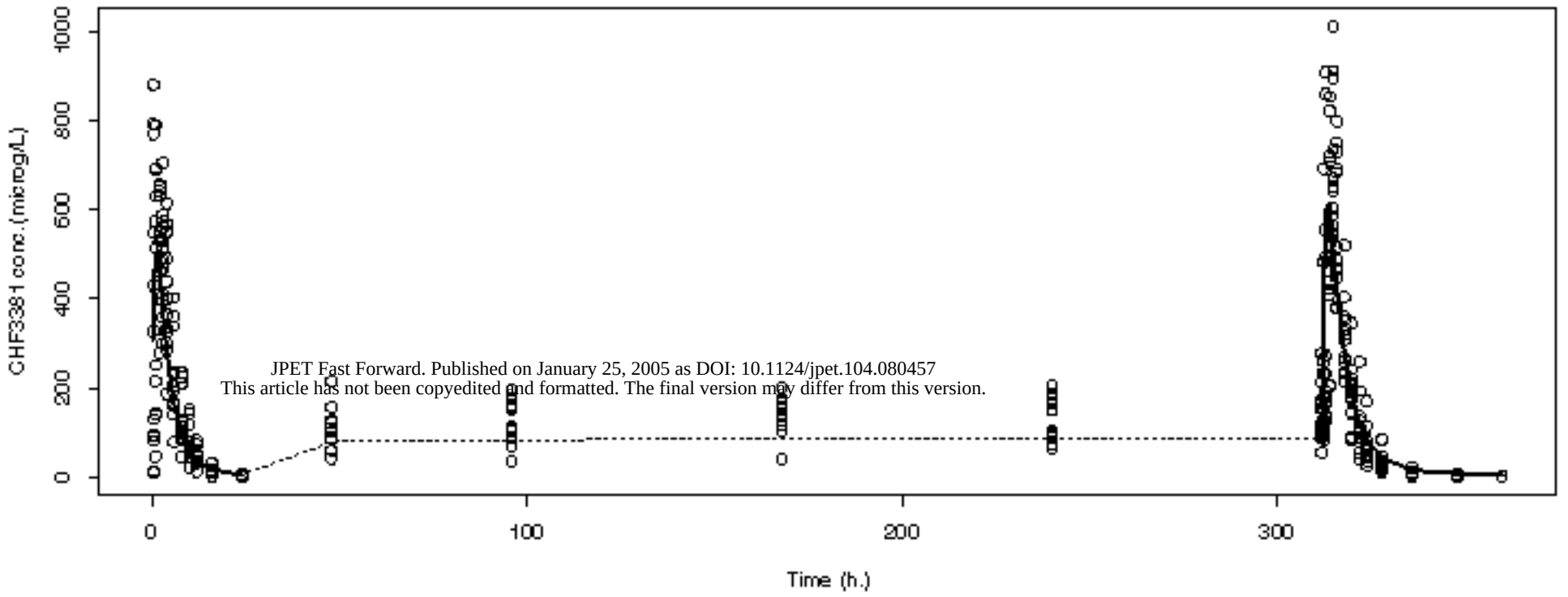

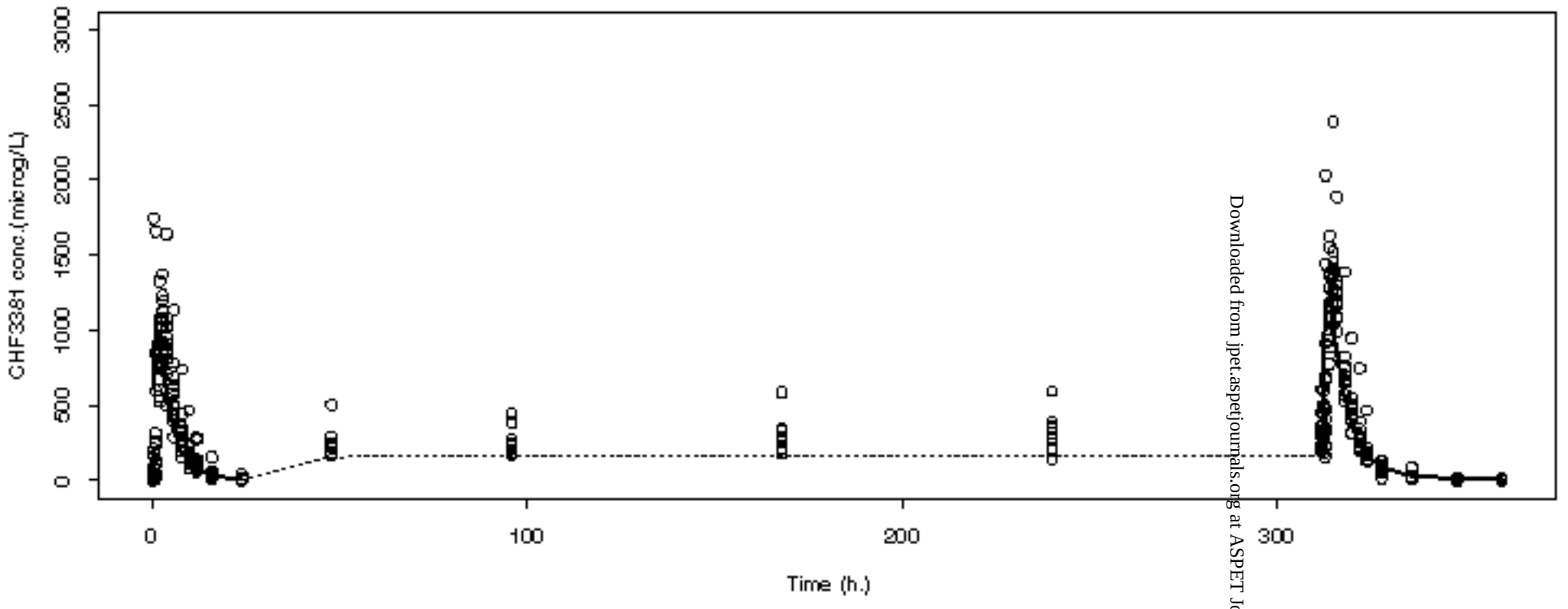

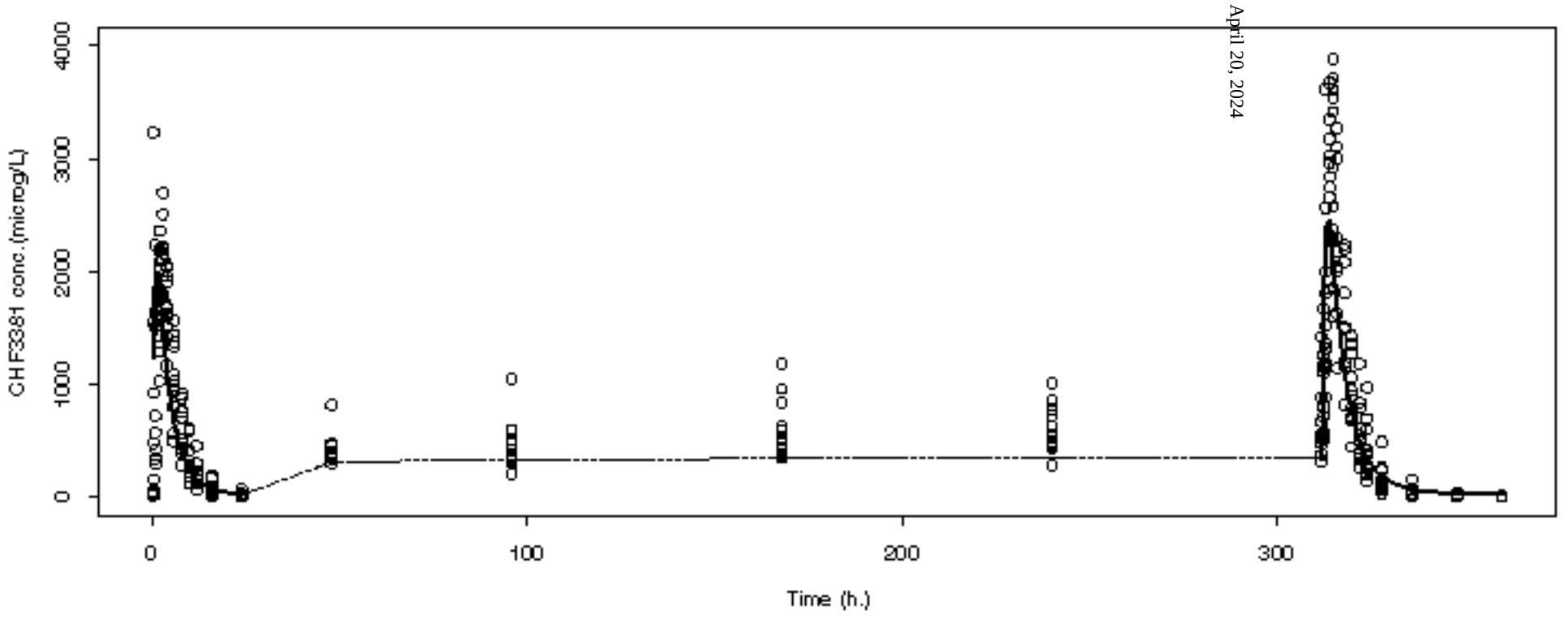

Figure 3

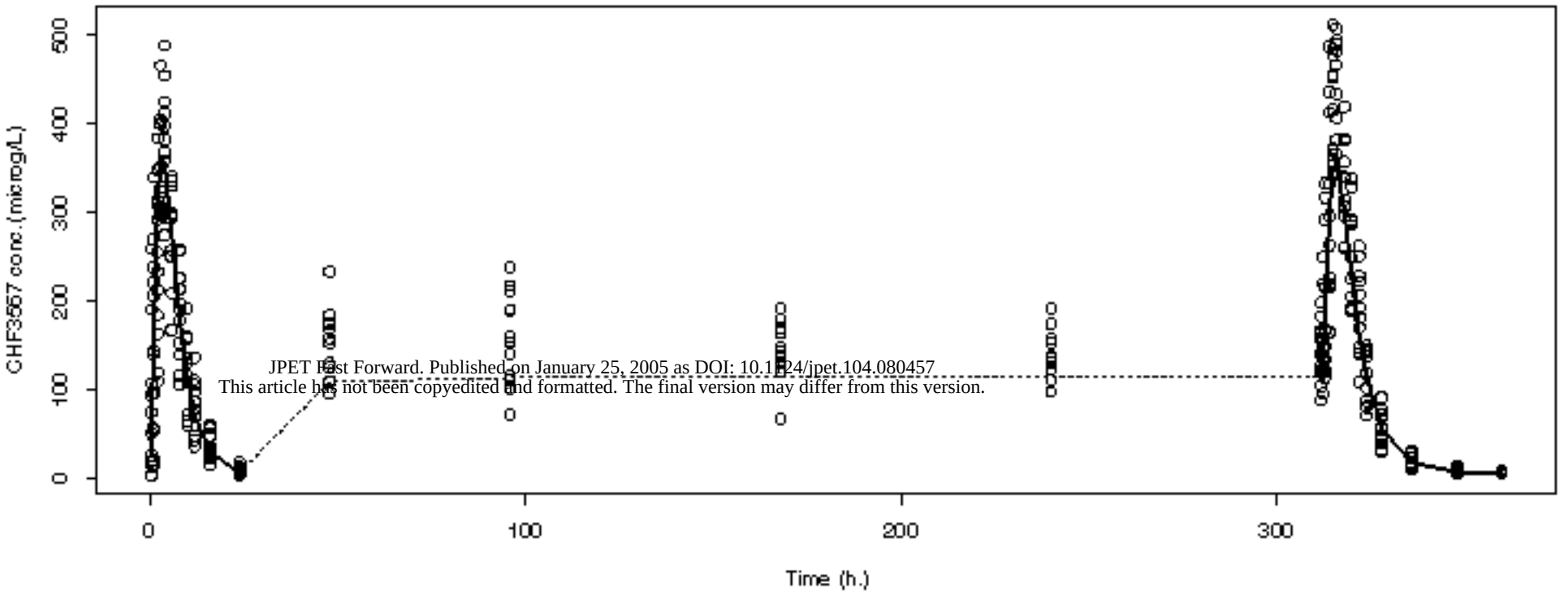

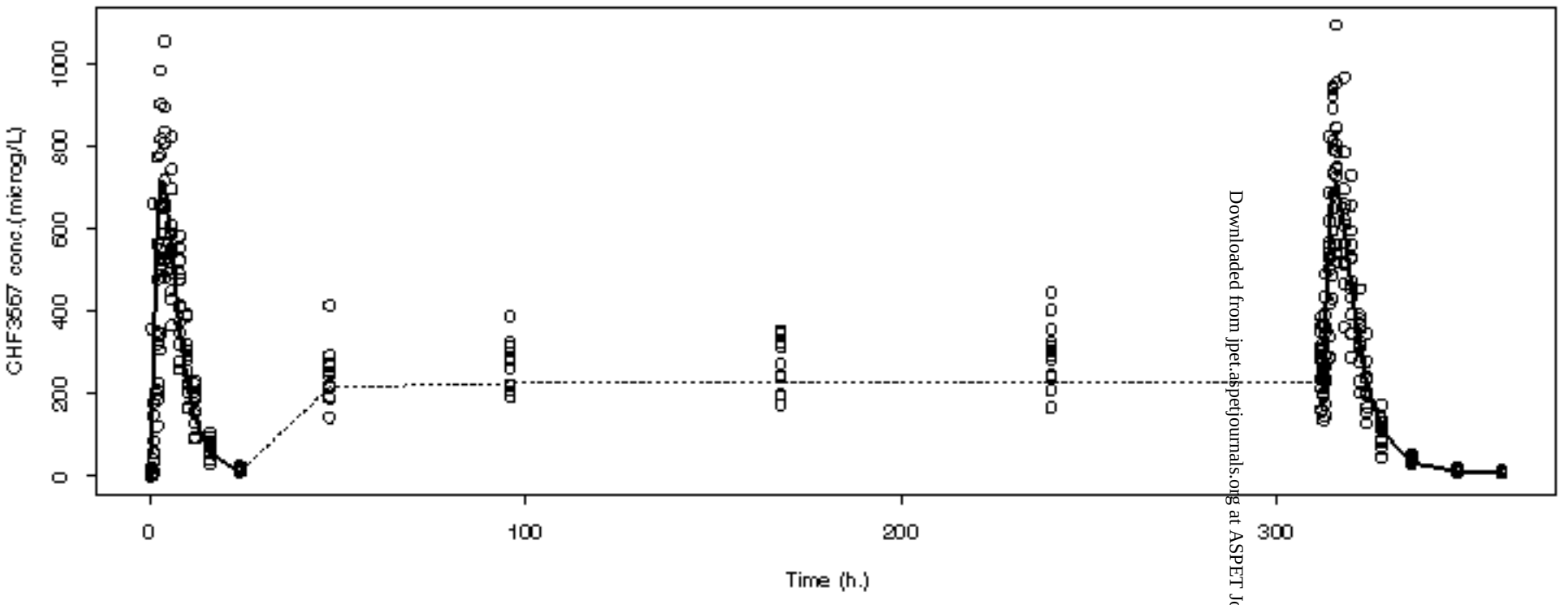

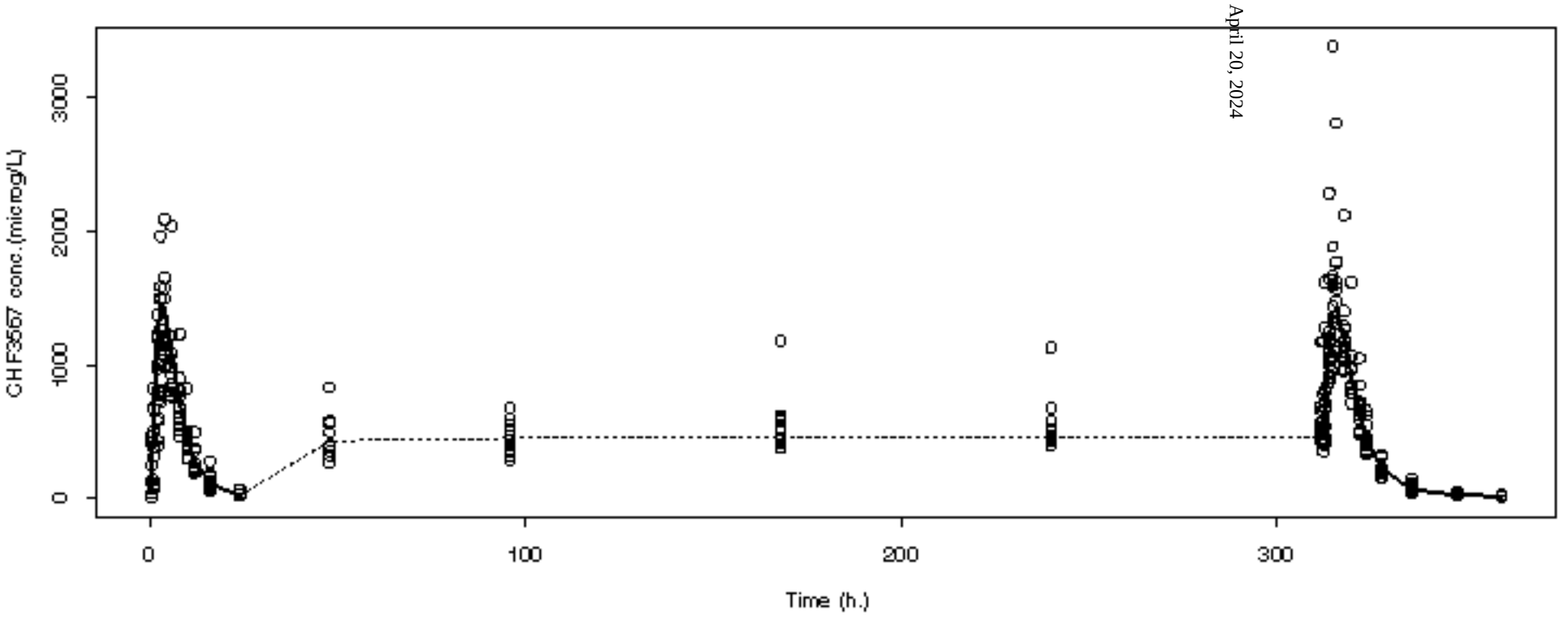

Figure 4

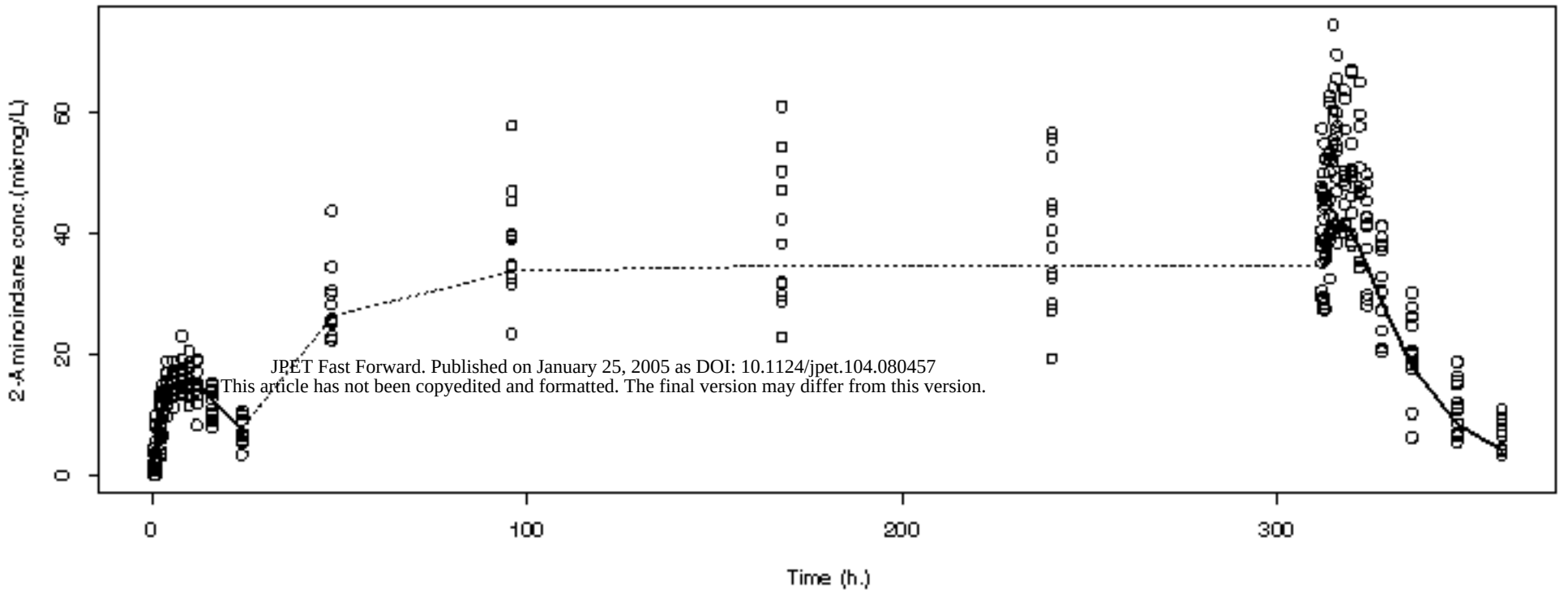

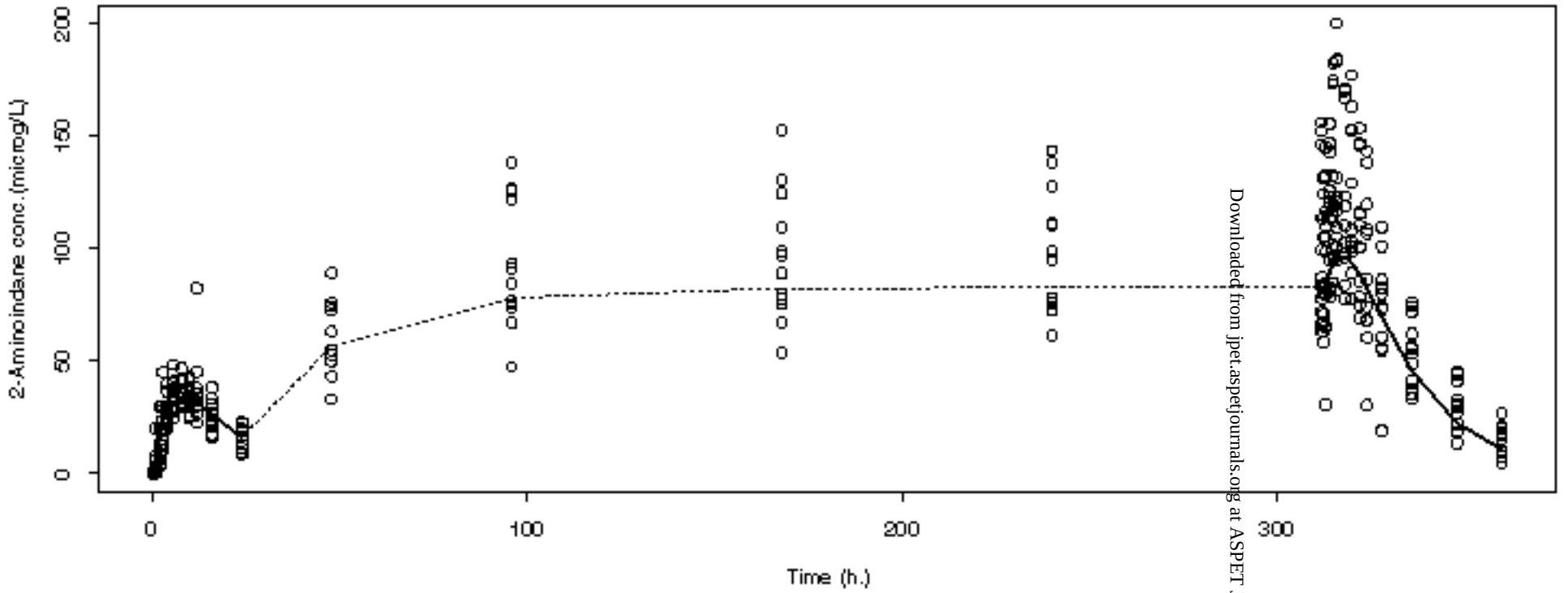

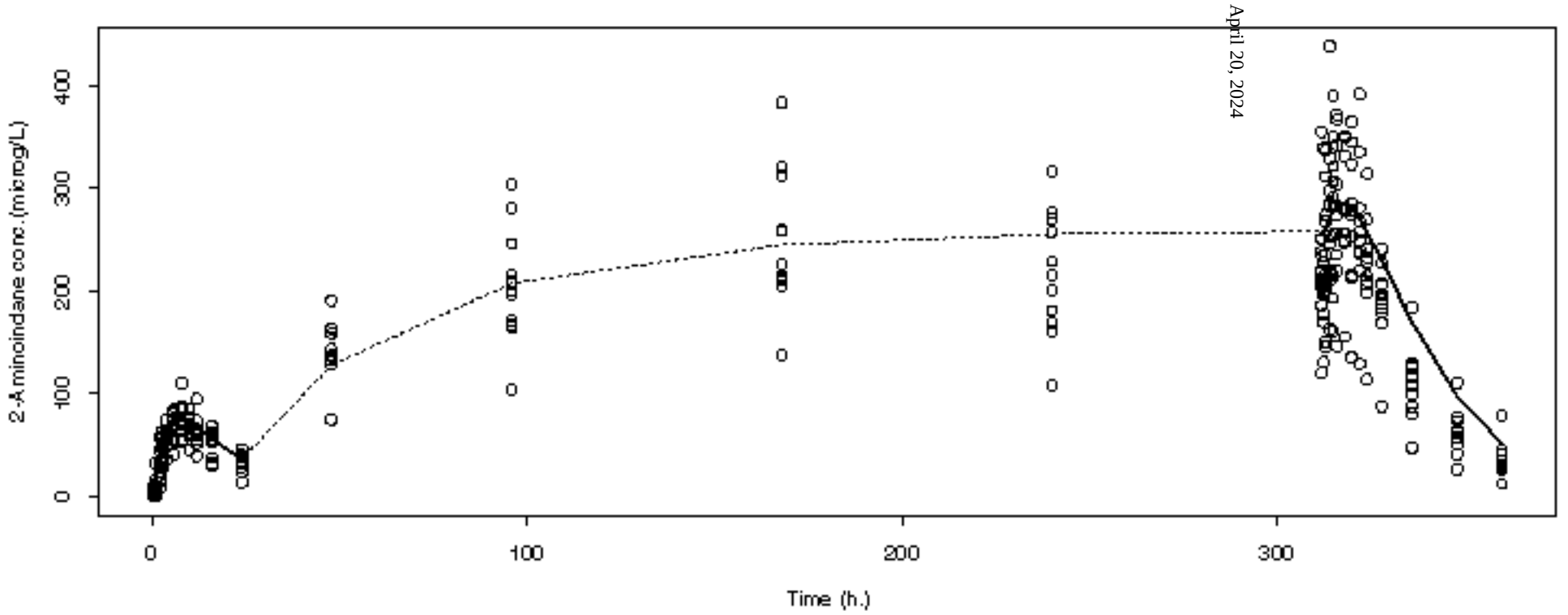

Figure 5

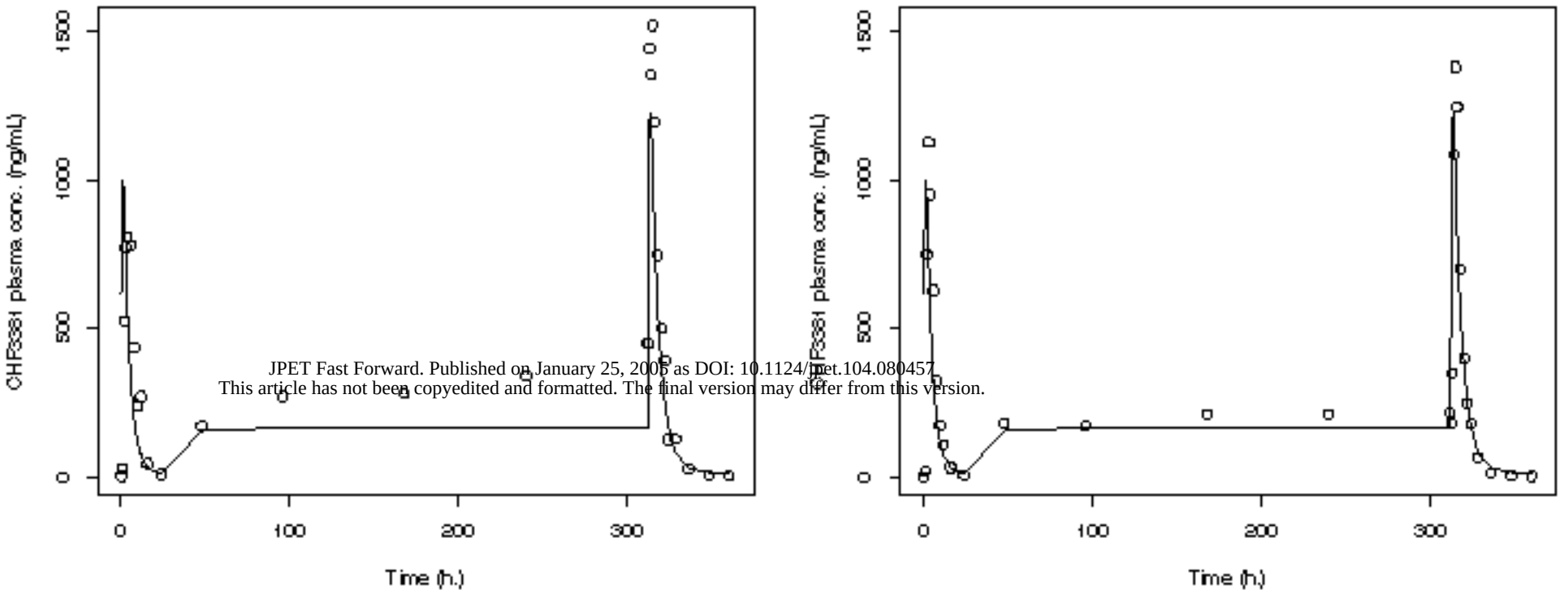

JPET Fast Forward. Published on January 25, 2005 as DOI: 10.1124/jpet.104.080457
This article has not been copyedited and formatted. The final version may differ from this version.

Figure 6

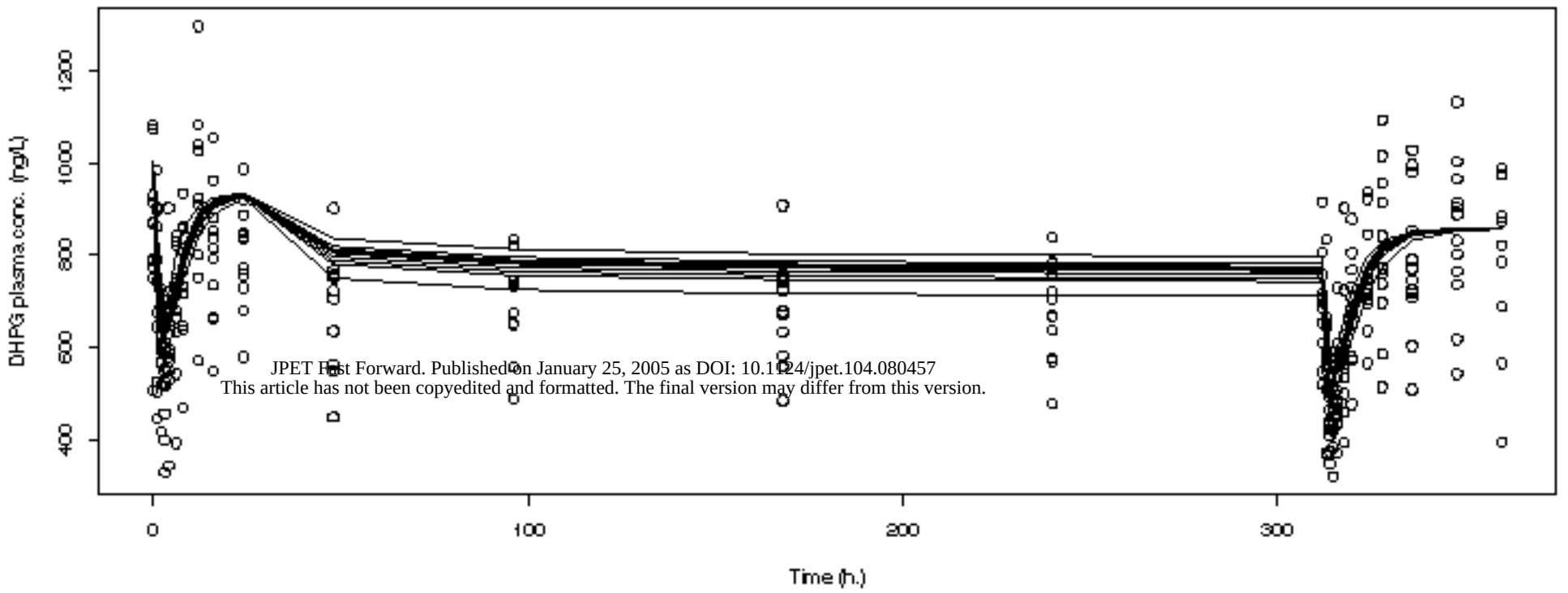

Figure 7